Reprinted from the Journal of the American Ceramic Society, Vol. 78, No. 4, April 1995

journal

J. Am. Ceram. Soc., 78 [4] 972-80 (1995)

Oxidation Kinetics of a Continuous Carbon Phase in a Nonreactive Matrix

Andrew J. Eckel*

National Aeronautics and Space Administration, Lewis Research Center, Cleveland, Ohio 44135

James D. Cawley*

Case Western Reserve University, Cleveland, Ohio 44106

Triplicane A. Parthasarathy*

UES, Inc., Dayton, Ohio 45432

Analytical solutions of and experimental results on the oxidation kinetics of carbon in a pore are presented. Reaction rate, reaction sequence, oxidant partial pressure, total system pressure, pore/crack dimensions, and temperature are analyzed with respect to the influence of each on an overall linear-parabolic rate relationship. Direct measurement of carbon recession is performed using two microcomposite model systems oxidized in the temperature range of 700° to 1200°C, and for times to 35 h. Experimental results are evaluated using the derived analytical solutions. Implications on the oxidation resistance of continuous-fiber-reinforced ceramic-matrix composites containing a carbon constituent are discussed.

I. Introduction

THE kinetics of carbon oxidation are critical for a broad range of materials systems, processes, and technologies. And, for the specific case of carbon oxidizing and receding in a nonreactive matrix, the kinetics can be either the Achilles' heel or an enabling step. For example, in a continuous-fiber-reinforced ceramic-matrix composite (CFCC), carbon may be present as the reinforcing fiber or as a thin film at the fiber–matrix interface. The interfacial layer provides the critically important debond layer which imparts to the composite superior mechanical properties—most importantly, fracture toughness. The loss of the carbon in these materials by oxidation severely reduces the service life and is potentially catastrophic. On the other hand, the complete removal of the continuous carbon phase constituent from a matrix may be desirable in material systems where, by design, the loss of "fugitive" carbon forms a beneficial void.[1] Thus, an understanding of the key parameters controlling the oxidation kinetics of a continuous carbon phase constituent is useful for the design and life prediction of several material systems.

The objective of this work was to answer some of the key oxidation questions associated with the technological exploitation and experimental evaluation of materials with a continuous carbon phase. Specifically, can a fiber-reinforced composite be designed with a carbon interphase thin enough to slow oxidation to a technologically acceptable rate? Why are the observed oxidation kinetics in composites coupled to stress? Do carbon oxidation kinetics depend on whether CO or CO_2 is formed? What is the influence of convection caused by product gases? Finally, what experimental variables must be controlled to design an experiment that accurately simulates the oxidation behavior for a given application?

Given its historical and current technological importance, the oxidation of bulk carbon, in its many varied forms, has been widely studied.[2–4] Surface reaction rates are known to be dependent on a variety of factors such as chemical composition, density, porosity and presence of surface defects, crystallinity, and crystallographic orientation. In all cases, the rates are rapid—in the range of 10^{-4} to 10^{-1} g/(cm^2·s) which corresponds to recession rates on the order of mm/h to mm/min) for 1 atm oxygen at 1000°C.

Studies on gas phase diffusion-limited oxidation kinetics have generally focused on one or a combination of the following three situations: (1) gas diffusion through continuous pores or cracks in a "protective" coating on a carbon substrate (e.g., coated carbon/carbon composites);[5–8] (2) pore/crack sealing by a condensed matrix-oxidation reaction product;[7–11] or (3) oxidation of a thin carbon film in a nonreactive matrix for a specific condition of interest.[12,13] Of particular relevance to the work that follows, prior studies have shown that 800°C is an important temperature when considering oxidation of carbon fiber-reinforced composites. At temperatures below 800°C, the rate of carbon recession is dominated by the kinetics of the chemical reaction at the receding carbon surface. In contrast, at temperatures greater than 800°C (but low enough that pore/crack sealing is not an issue), gas phase diffusion assumes an increasingly important role in determining kinetics. This paper generalizes oxidation of thin carbon films and fibers in nonreactive matrices with a formal analysis, explicitly including both chemical reaction and gas phase diffusion effects. The resulting general model for oxidation kinetics provides the basis for evaluating other limiting cases.

In the following section, a comprehensive analytical model is developed using reaction rate formalism and kinetic theory of gases. The results of two sets of experiments are then interpreted using aspects of this model in Section III. In the experiments, recession distance is measured directly, using either metallography or precise measurements of dimensional changes. This is in contrast to most oxidation studies, where oxidation rate is measured indirectly, i.e., through degradation in mechanical properties, weight changes, or changes in electrical resistivity.[3,13,14] The advantage of directly measuring carbon recession is that it provides the opportunity to validate the assumptions used in derivation of the model.

R. J. Kerans—contributing editor

Manuscript No. 193677. Received April 12, 1994; approved November 14, 1994.
Supported in part by the Ohio Aerospace Institute (CCRP 93-1-027) and a NASA/CWRU cooperative agreement on ceramic processing (NCC3-139).
*Member, American Ceramic Society.

II. Modeling of the Oxidation Process

The variables affecting the rate of carbon oxidation include the kinetics of the oxidation reaction occurring at the carbon surface, the characteristic dimension of the carbon (the fiber diameter or the coating thickness), the nature of the reaction product (either CO or CO_2), the molecular weight of the gases, the temperature, and the total ambient pressure. One advantage of a rigorous analysis is that the sensitivity of the oxidation process to each of these variables can be assessed. The analysis focuses on obtaining an expression for the carbon recession rate. In all cases, it is assumed that the dense and homogeneous carbon initially occupies a well-defined volume which is finite in the two directions which are perpendicular to the oxidation direction and infinite in the direction parallel to the oxidation direction, as shown schematically in Fig. 1. The results of the model are equally applicable to the oxidation of a carbon fiber (in a carbon-fiber-reinforced CFCC) and a carbon coating (for example, the fiber/matrix interface coating in a silicon carbide-fiber-reinforced composite). The discussion below is limited to the oxidation of a thin annulus of carbon between a nonreactive fiber and matrix. For silicon-based CFCCs, oxidation of both the fiber and matrix can be neglected at "intermediate" temperatures (less than ≈1000°C). This assumption has been used because it has been shown that oxidative damage is most severe in this intermediate temperature range.[14,15] It is also assumed that the receding carbon maintains a planar interface.

The assumption is made that the oxidation of carbon is governed by sequential linear-parabolic kinetics, i.e., the recession distance, x, is related to the oxidation time, t, by[16]

$$x^2/k_p + x/k_l = t \tag{1}$$

where k_p is termed the parabolic rate constant (m^2/s) and k_l the linear rate constant (m/s). When the recession distance is small, the left-hand side of Eq. (1) is dominated by the linear term, but as the recession distance increases there will always be a transition to parabolic kinetics. It is common to refer to the former as reaction control and to the latter as diffusion control, although some diffusion-controlled processes give linear kinetics and some reaction-controlled processes are nonlinear. In the analysis that follows, the two limiting cases are treated independently in order to isolate the importance of system variables on each.

(1) Reaction-Controlled Kinetics

In this case, the reaction at the receding carbon interface is assumed to be first order, and either

$$O_2 + C \leftrightarrow CO_2 \tag{2a}$$

or

$$O_2 + 2C \leftrightarrow 2CO \tag{2b}$$

The rate of the reaction, r ($mol/m^2 \cdot s$), is given by

$$r = K_r c_\xi \tag{3}$$

where K_r is the reaction rate constant (m/s) for the oxidation reaction and c_ξ is the concentration of oxygen (mol/m^3) at $x = \xi$ (see Fig. 1). If it is appropriate to consider the diffusive supply of oxygen to be infinitely fast, then c_ξ is effectively equal to c_O, the concentration of oxygen in the atmosphere. c_O can be alternately written as χc_T, where χ is the oxidant partial pressure and c_T is the total concentration of gas molecules the atmosphere (mol/m^3). In this case, the carbon reces rate is constant (i.e., independent of time) and so-called li kinetics are observed, i.e.,

$$d\xi/dt = k_l$$

Equivalently,

$$\xi = k_l t \tag{5}$$

if no recession has occurred prior to $t = 0$. The linear rate constant can be written as

$$k_l = K_r \chi c_T / N \tag{6}$$

where N is the molar density of carbon (mol/m^3). The reaction rate constant is conventionally written using an Arrhenius form, and c_T can be written using the ideal gas law. Thus, an alternate expression for k_l, in terms of fundamental quantities, is

$$k_l = (1/N)(\chi P/RT) k_0 \exp(-Q/RT) \tag{7}$$

where k_0 is a constant (m/s), Q is the activation energy (J/mol), P is the pressure (Pa), R is the gas constant (J/mol·K), and T is absolute temperature (K). Values for N, k_0 and Q are dependent on the nature of the carbon and must be determined experimentally. There is a wide variation in the reported values for oxidation rates of bulk carbon.[2,3] Assuming these experimentally determined values are constant over the temperature range of interest, the functional dependence of temperature and pressure on the linear oxidation rate can be predicted from Eq. (7). For pressure, the oxidation rate is expected to vary linearly. The temperature dependence is readily observed by considering the product of the linear rate constant times temperature, or

$$k_l T \propto \exp(-Q/RT) \tag{8}$$

When the argument of the exponential function is small (e.g., activation energy is much less than the product RT) the $k_l T$ product approaches a constant value, i.e., inverse linear dependence. On the other hand, when the exponential argument is large, the reaction rate increases exponentially with increasing temperature.

(2) Diffusion-Controlled Kinetics

In this case, the reaction at the carbon interface is assumed to be infinitely fast, but several distinct reaction sequences are still possible and affect mass transport. For example, the case of simultaneous oxidation of carbon and silicon carbide in CFCCs was considered in a recent set of papers. Two cases were analyzed: O_2 diffusion in and CO_2 diffusion out, and O_2 diffusion in and CO diffusion out.[9] It is also possible for CO formed at the carbon interface to undergo a secondary oxidation to form CO_2. This case has also been analyzed.[12] The gas concentration profiles in a crack/pore for each of the three reaction sequence cases are shown in Figs. 2(a), (b), and (c). All three will be considered here. It should be noted that although only one reaction sequence can be the correct description for a particular situation, it is plausible that different sequences will occur under different conditions.

It greatly simplifies the analysis to treat the diffusion coefficients of all of the species in the gas phase as identical in magnitude. This is not strictly true, but the differences are small, as discussed below.

Gas phase diffusion coefficients can be predicted using Chapman–Enskog theory. The expression for the diffusion coefficient of gas A, in a stationary atmosphere of B, is[17]

$$D_{AB} = 5.9543 \times 10^{-24} [(1/M_A) + (1/M_B)]^{1/2} T^{3/2} / (P\sigma_{AB}{}^2 \Omega_{AB}) \tag{9}$$

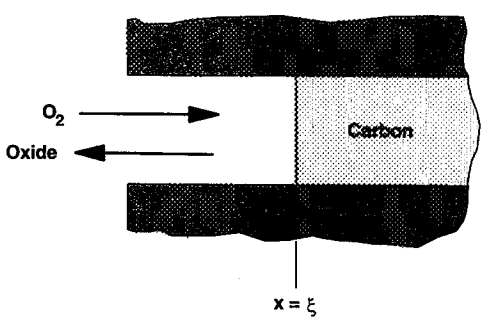

Fig. 1. Schematic of carbon recession during oxidation in a nonreactive matrix.

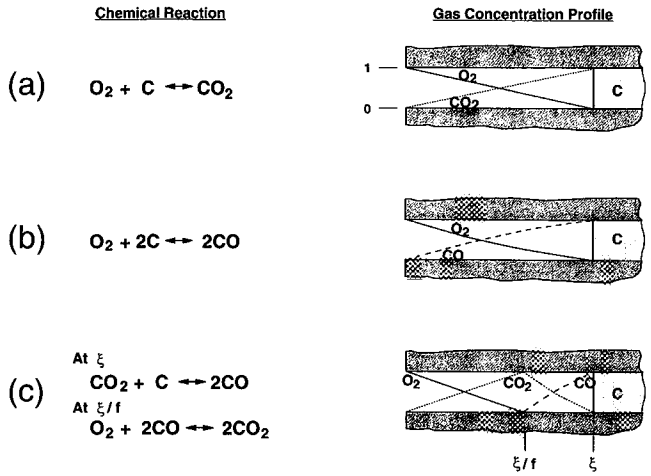

Fig. 2. Plausible oxidation reaction sequences: (a) O_2 diffusion in and CO_2 diffusion out, (b) O_2 diffusion in and CO diffusion out, (c) CO formation at the carbon surface with subsequent oxidation to CO_2.

where D is the diffusivity (m^2/s), T is the absolute temperature (K), M is the molecular weight (kg/mol), P is the total pressure (Pa), σ is the collision diameter (m), and Ω is a tabulated integral which is a function of the energy of molecular interaction parameter, ε (typically tabulated as a ratio to Boltzmann's constant, k). For mixtures, the effective collision diameter and energy of interaction are given by

$$\sigma_{AB} = (\sigma_A + \sigma_B)/2 \tag{10}$$

and

$$\varepsilon_{AB}/k = [(\varepsilon_A/k)(\varepsilon_B/k)]^{1/2} \tag{11}$$

respectively. Inspection of Eqs. (9), (10), and (11) indicates that $D_{AB} = D_{BA}$. For the cases under consideration here, it is convenient to examine the ratio D_{AB}/D_{AC} where A, B, and C refer to different gas species. With Eq. (9) it is possible to express this ratio as

$$D_{AB}/D_{AC} = \{[M_C(M_A + M_B)]/[M_B(M_A + M_B)]\}^{1/2} [(\sigma_A + \sigma_C)/(\sigma_A + \sigma_B)]^2 (\Omega_{AC}/\Omega_{AB}) \tag{12}$$

The relevant parameters for the systems of interest are given in Table I. Ignoring the slight temperature dependence of Ω, and substituting these values into Eq. (12) yields $D_{CO,O_2}/D_{CO,CO_2} = 1.28$, $D_{O_2,CO}/D_{O_2,CO_2} = 1.30$, and $D_{CO_2,O_2}/D_{CO_2,CO} = 0.99$. The temperature dependence of Ω changes these ratios by less than 1% over the temperature range of interest (800°–1200°C). In other words, the diffusion coefficients vary by less than 30%, even in the most extreme cases.

Conservation of the oxidant proves to be the most convenient frame of reference for most of the discussion. It is shown that the solution for the most complex case, CO formation with subsequent oxidation to CO_2, is just a combination of the two simpler solutions for CO and CO_2 as single reaction products. Further generalization to include Knudsen effects (i.e., gas diffusion limited by dimensions of the channel) is then offered.

(A) O_2 Diffusion In and CO_2 Diffusion Out: It is assumed that the concentration of the oxidant at the surface, $x = 0$, is fixed by the composition of the atmosphere to be χc_T and the concentration at the interface, $x = \xi$, is fixed by the appropriate phase equilibria (Eq. (2*a*)) to be c_ξ. It is further assumed that the quasi steady state exists, i.e., the flux density of oxygen, j_{ox}, is not a function of position at any time t. The geometrical arrangement is schematically illustrated in Fig. 2(a). The flux density of oxygen over the domain $0 < x < \xi$ may be, in general, written[18]

$$j_{ox} = -D\,\partial c_{ox}/\partial x + v^* c_{ox} \tag{13}$$

where v^* is the molar average velocity, which may be defined using

$$v^* = (\Sigma c_i v_i)/(\Sigma c_i) \tag{14}$$

where v_i is the velocity of the ith species with respect to a stationary coordinate system. By definition

$$j_i = c_i v_i \tag{15}$$

so that Eq. (14) can be rewritten, in the general form, as

$$v^* = \Sigma(j_i)/c_T \tag{16}$$

where c_T is the total concentration of gas molecules, which is a constant. For this particular case, where c_T is simply the sum of the concentrations of oxygen and carbon monoxide, Eq. (16) becomes

$$v^* = (j_{ox} + j_{co_2})/c_T \tag{17}$$

Substituting Eq. (17) into Eq. (13) yields

$$j_{ox} = -D\,\partial c_{ox}/\partial x + (c_{ox}/c_T)(j_{ox} + j_{co_2}) \tag{18}$$

Conservation of mass requires

$$j_{co_2} = -j_{ox} \tag{19}$$

and therefore $v^* = 0$ and Eq. (13) simplifies to Fick's first law

$$j_{ox} = -D\,\partial c_{ox}/\partial x \tag{20}$$

Assuming quasi steady state yields a linear concentration gradient, which, upon integration gives

$$j_{ox} \approx -D(c_{ox}(\xi) - c_{ox}(0))/\xi \tag{21}$$

The recession rate is given by mass balance; i.e., the thickness removed is equal to the negative of the flux density of carbon away from the interface divided by the molar density of carbon, N, (mol/m^3) in the condensed state, or,

$$d\xi/dt = -j_{co_2}/N \tag{22}$$

Substituting Eqs. (19) and (21) into (22) gives a standard form for parabolic kinetics

$$d\xi/dt = [D(c_{ox}(0) - c_{ox}(\xi))]/(N\xi) \tag{23}$$

and integrating gives

$$\xi^2 = [2D(c_{ox}(0) - c_{ox}(\xi))/N]t \tag{24}$$

which can be written in familiar notation as

$$\xi = k_p^{1/2} t^{1/2} \tag{25}$$

Table I. Parameters Used in Calculation of Gas Phase Diffusion Coefficients Using Chapman–Enskog Theory*

Gas	M (kg/mol)	σ (m)	ε/k (K)	Mixture	$\sqrt{[(\varepsilon_i/k)(\varepsilon_j/k)]}$ (K)	Ω_{AB} (at 1073 K)
O_2	32×10^{-3}	3.467×10^{-10}	106.7	O_2/CO	99	0.737
CO	28×10^{-3}	3.690×10^{-10}	91.7	CO/CO_2	144	0.784
CO_2	44×10^{-3}	3.941×10^{-10}	195.2	CO_2/O_2	134	0.774

*Values for Ω are interpolated from tabulated values.[17]

with k_p, termed the parabolic rate constant, given by

$$k_p = [2D(c_{ox}(0) - c_{ox}(\xi))/N] \tag{26}$$

(B) O_2 Diffusion In and CO Diffusion Out: In this case it is assumed that reaction (2*b*) occurs at $x = \xi$ and that the CO diffuses, without reaction, to the external surface of the pore. This is plausible, since it is well known that CO may be maintained as a metastable species for long times. The concentration gradients for this case are illustrated in Fig. 2(b). The chemical reaction in this case produces two moles of gaseous product, CO, for every mole of gaseous reactant, O_2, consumed, i.e.,

$$j_{co} = -2j_{ox} \tag{27}$$

which makes the convection term in Eq. (13) nonzero. Substituting Eq. (27) into Eq. (16) and in turn into Eq. (13) yields, upon rearrangement,

$$j_{ox} = -[(Dc_T)/(c_T + c_{ox})]\ \partial c_{ox}/\partial x \tag{28}$$

Integration of this expression does not yield a linear concentration gradient. The assumption of quasi steady state, i.e., j_{ox} is not a function of position at any time t, allows the right-hand side of Eq. (28) to be set equal to a constant

$$A = -[Dc_T/(c_T + c_{ox})]\ \partial c_{ox}/\partial x \tag{29}$$

Since $\partial(c_T + c_{ox})/\partial x = \partial c_{ox}/\partial x$, this may be rearranged to give

$$\partial[\ln (c_T + c_{ox})]/\partial x = A' \tag{30}$$

and upon integration

$$\ln (c_T + c_{ox}) = A'x + B \tag{31}$$

or

$$c_{ox} = B' \exp(A'x) - c_T \tag{32}$$

Given the boundary conditions

$$c_{ox}(x = 0,t) = c_{ox}(0) \tag{33}$$

$$c_{ox}(x = \xi,t) = c_{ox}(\xi) \tag{34}$$

the constants can be evaluated to give

$$c_{ox} = (c_T + c_{ox}(0)) \exp\{\ln [(c_T + c_{ox}(\xi))/(c_T + c_{ox}(0))](x/\xi)\} - c_T \tag{35}$$

Upon substitution into Eq. (28), this yields

$$j_{ox} = -(Dc_T/\xi) \ln [(c_T + c_{ox}(\xi))/(c_T + c_{ox}(0))] \tag{36}$$

The rate of carbon recession in this case is

$$d\xi/dt = -j_{co}/N = 2j_{ox}/N \tag{37}$$

Substituting Eq. (36) and integrating yields

$$\xi^2 = (4Dc_T/N) \ln [(c_T + c_{ox}(0))/(c_T + c_{ox}(\xi))]t \tag{38}$$

The kinetics remain parabolic, but the parabolic rate constant, k_p', is now defined as

$$k_p' = (4Dc_T/N) \ln [c_T + c_{ox}(0))/(c_T + c_{ox}(\xi))] \tag{39}$$

or equivalently

$$k_p' = (4Dc_T/N) \ln [(1 + (c_{ox}(0)/c_T))/(1 + c_{ox}(\xi)/c_T))] \tag{40}$$

(C) Formation of CO at Receding Carbon Surface with Subsequent Oxidation to CO_2: In this case it is assumed that the atmosphere is pure O_2 and that CO is formed at the receding surface. Following the analysis of Bernstein and Koger,[12] the CO is oxidized to form CO_2 at a position ξ/f, where f is a constant. The relevant chemical reactions are

$$CO_2 + C \rightarrow 2CO \qquad \text{at } x = \xi \tag{41}$$

and

$$2CO + O_2 \rightarrow 2CO_2 \qquad \text{at } x = \xi/f \tag{42}$$

The concentration gradients of the gaseous species are schematically illustrated in Fig. 2(c). The previous analysis was from the (valid) point of view of continuity of carbon flux.[12] The analysis given below focuses on the flux of oxidant, in this case CO_2, and is intended to illustrate that this problem is a straightforward extension of the two simpler cases given in Sections II(2)(A) and II(2)(B). It is convenient to divide the problem into two regions: Region I includes the domain $0 \le x \le \xi/f$; and Region II is defined by $\xi/f \le x \le \xi$. Note that if $f = 1$ then Region I covers the entire range $0 \le x \le \xi$, and the system is equivalent to that presented in II(2)(A), and if $f = \infty$ then the entire spatial domain falls into Region II and the case discussed in II(2)(B) applies.

In Region I, carbon dioxide is the oxidant and its flux is described in a manner analogous to Eq. (13), giving

$$j_{co_2} = -D\ \partial c_{co_2}/\partial x + v^* c_{co_2} \tag{43}$$

but this again simplifies to Fick's first law. The reasoning for setting v^* equal to zero in this case is that although reaction (41) consumes 1 mol of gaseous reactant to make 2 mol of gaseous product, this "extra" mole is consumed in reaction (42), which yields only 2 mol of gaseous products from 3 mol of reactants. Effectively, there is a negative convective term at $x = \xi$ which is balanced by a positive convective term of equal magnitude at $x = \xi/f$. Therefore, quasi steady state again yields a linear concentration gradient and

$$j_{co_2} = -D[c_{co_2}(\xi/f) - c_{co_2}(0)]/(\xi/f) \tag{44}$$

and since

$$d\xi/dt = -j_{co_2}/N \tag{45}$$

substitution and integration yields

$$\xi^2 = (2Df/N)[c_{co_2}(\xi/f) - c_{co_2}(0)]t \tag{46}$$

yielding a parabolic rate constant, k_p'', for this case

$$k_p'' = (2Df/N)[c_{co_2}(\xi/f) - c_{co_2}(0)] \tag{47}$$

which involves the unknown "f".

Turning attention to Region II, j_{co_2} is given by Eq. (43), but in this case v^* is nonzero and analogous to Eq. (28). Substitution for v^* using fluxes, in this case j_{co_2} and j_{co}, and rearranging, gives

$$j_{co_2} = -[(Dc_T)/(c_T + c_{co_2})]\ \partial c_{co_2}/\partial x \tag{48}$$

Applying the assumption of quasi steady state and the following boundary conditions

$$c_{co_2}(x = \xi/f,t) = c_{co_2}(\xi/f) \tag{49}$$

$$c_{co_2}(x = \xi,t) = c_{co_2}(\xi) \tag{50}$$

gives

$$c_{co_2} = (c_{co_2}(\xi) + c_T) \exp\{[f/(f-1)] \ln [(c_T + c_{co_2}(\xi))/(c_T + c_{co_2}(\xi/f))]\ (x/\xi - 1)\} - c_T \tag{51}$$

Substitution of Eq. (48) into Eq. (45) and rearrangement yields

$$j_{co_2} = -(Dc_T/\xi)[f/(f-1)] \ln [(c_T + c_{co_2}(\xi))/(c_T + c_{co_2}(\xi/f))] \tag{52}$$

Now, for the case of this reaction sequence, the recession rate is given by

$$d\xi/dt = -1/2j_{co}/N = j_{co_2}/N \tag{53}$$

The origin of the one-half in Eq. (53) comes from the fact that only one of the CO molecules on the right-hand side of reaction (41) removes a carbon from the condensed carbon. Substitution of (52) in (53) and integration yields

$$\xi^2 = (2Dc_T/N)[f/(f-1)] \ln[(c_T + c_{co_2}(\xi/f))/(c_T + c_{co_2}(\xi))]t \quad (54)$$

and an alternate form for the parabolic rate constant, k_p''

$$k_p'' = (2Dc_T/N)[f/(f-1)] \ln[(c_T + c_{co_2}(\xi/f))/(c_T + c_{co_2}(\xi))] \quad (55)$$

Equating Eqs. (47) and (55) and solving for "f" yields

$$f = [c_T/(c_{co_2}(\xi/f) - c_{co_2}(0))] \ln[(c_T + c_{co_2}(\xi/f))/(c_T + c_{co_2}(\xi))] + 1 \quad (56)$$

and substituting back into either (47) or (55) allows "f" to be eliminated from the expression for the parabolic rate constant,

$$k_p'' = (2D/N)\{c_T \ln[(c_T + c_{co_2}(\xi/f))/(c_T + c_{co_2}(\xi))] + [c_{co_2}(\xi/f) - c_{co_2}(0)]\} \quad (57)$$

(D) Comparison of the Parabolic Rate Constants: At first inspection, Eqs. (26), (40), and (57) appear quite different. However, referring to the schematics (Figs. 2(a–c)) illustrates how these may be simplified and compared. For the case of O_2 diffusion in and CO_2 diffusion out, $c_{ox}(0) \approx \chi c_T$ and $c_{ox}(\xi) \approx 0$ so that

$$k_p \approx 2\chi(Dc_T/N) \quad (58)$$

Similarly, for the case of O_2 diffusion in and CO diffusion out, $c_{ox}(0) \approx \chi c_T$ and $c_{ox}(\zeta) \approx 0$, so that

$$k_p' \approx 4 \ln[1 + \chi](Dc_T/N) \quad (59)$$

Finally, for the case of CO formation at receding carbon surface with subsequent oxidation to CO_2 at ξ/f, setting $c_{co_2}(\xi/f) \approx \chi c_T$, $c_{co_2}(0) \approx 0$ and $c_{co_2}(\xi) \approx 0$ yields

$$f = 1 + (1/\chi) \ln(1 + \chi) \quad (60)$$

and

$$k_p'' \approx 2[\chi + \ln(1 + \chi)](Dc_T/N) \quad (61)$$

Equations (58), (59), and (61) differ only in the magnitude of the numerical constants which precede the common Dc_T/N factor. It is interesting to compare their magnitudes and reflect on their physical interpretation.

O_2 diffusion in and CO_2 diffusion out yields the slowest kinetics for all values of χ. O_2 diffusion in and CO diffusion out predicts kinetics which are more rapid, but only modestly. For example, for 1 atm pure O_2 ($\chi = 1$), $k_p'/k_p \approx 1.39$. Mass balance would suggest that the formation of CO would remove carbon twice as fast as the formation of CO_2, since 2 mol of carbon would be removed for each mole of oxygen which diffuses in. The net increase, however, is only 39%, because the convection caused by the outward flow of CO opposes diffusion of the oxidant. This modest increase in oxidation kinetics would be further reduced when the additional effect of variation in the gas phase diffusion coefficients, Eq. (12), is taken into account. For example, if one assumed no gradients (maximum effect), the ratio k_p'/k_p becomes nearly unity.

The formation of CO with subsequent oxidation to CO_2 yields a prediction of the most rapid kinetics, for 1 atm pure O_2. Still, the differences are small; $k_p''/k_p \approx 1.69$ and $k_p''/k_p' \approx 1.22$ (ignoring diffusion coefficient variations). It may seem counter-intuitive for this case to yield the most rapid kinetics, since a global mass balance states that only 1 mol of carbon will be removed for each mole of oxygen. The physical reason for the fast kinetics is that the existence of two regions yields steeper concentration gradients, for all species, at a given recession distance. This is illustrated by comparing Figs. 2(a), (b), and (c). Faster recession occurs because the kinetics of carbon recession are directly proportional to the flux of oxidant, which, in turn, is directly proportional to the oxygen concentration gradient.

(3) Knudsen Effects

The calculations carried out in Section II(2) involved the implied assumption that gas phase diffusion was determined by intermolecular collisions (Eq. (9)), which is sometimes termed "molecular diffusion." It is plausible that if carbon is present as either very small-diameter fibers or very thin interlayers, gas phase diffusion will be affected by collisions between molecules and the walls of the pore left by the receding carbon. The limiting case where molecule–wall collisions are much more frequent than intermolecular collisions is termed "Knudsen diffusion," and is characterized by a significantly smaller diffusion coefficient.

It is perhaps most useful to analyze the transition case, which is general, and take limiting cases to recover the expressions appropriate for the molecular and Knudsen regimes. An existing analysis may be readily extended to yield the parabolic rate constant for this case.[17] For the direct formation of CO_2, Section II(2)(A), the Knudsen case yields a parabolic rate constant of form identical to Eq. (26) except that an effective diffusion coefficient, D_{eff}, must be used. D_{eff} is given by

$$1/D_{eff} = 1/D + 1/D_k \quad (62)$$

It is trivial to take the limiting cases.

Both of the other plausible reaction sequences involve the formation of CO at the receding interface. Since the premise of the analysis is that intermolecular collisions are rare events, it is assumed that the case analyzed in II(2)(B), i.e., CO diffusion out without subsequent reaction, applies, and this is the case analyzed here. It is also possible to extend the analysis to include the case of CO formation with subsequent reaction to CO_2, but we have elected not to, since it is unlikely that gas phase equilibrium will be attained over distances of interest in CFCC's.

An expression has been derived[17] which describes the flux density of a species in a binary gas mixture in the transition regime, which may be written in the notation used here as

$$j_{ox} = -c_T/[((1 - \alpha c_{ox})/D) + (1/D_k)]\, \partial c_{ox}/\partial x \quad (63)$$

where D_k is the Knudsen diffusion coefficient which, for a cylindrical pore, can be calculated using[17]

$$D_k = 1.534d\sqrt{(T/M)} \quad (64)$$

where d is the diameter of the pore (m), T is absolute temperature (K), and M is molecular weight (kg/mol). D_k for an annular pore of thickness d' (such as would be left by a receding interlayer) would be modestly larger, because the average distance between collisions would be larger than d.

The parameter α in Eq. (63) is dependent on the relationship between the fluxes of the two species. For the oxidation case being analyzed here,

$$\alpha = 1 + j_{co}/j_{ox} \quad (65)$$

and, by Eq. (27), $\alpha = -1$, so that Eq. (63) is simply

$$j_{ox} = -c_T/[((1 + c_{ox})/D) + (1/D_k)]\, \partial c_{ox}/\partial x \quad (66)$$

Substitution in Eq. (37), integrating and rearranging gives

$$\xi^2 = (4Dc_T/N) \ln\{[(1 + c_{ox}(0)/c_T)(D_k/D) + 1]/[(1 + c_{ox}(\xi)/c_T)(D_k/D) + 1]\}t \quad (67)$$

The generalized expression for k_p' is therefore

$$k_p' = (4Dc_T/N) \ln\{[(1 + c_{ox}(0)/c_T)(D_k/D) + 1]/[(1 + c_{ox}(\xi)/c_T)(D_k/D) + 1]\} \quad (68)$$

or equivalently

$$k_p' = (4Dc_T/N) \ln\{[(1 + c_{ox}(0)/c_T) + (D/D_k)]/[(1 + c_{ox}(\xi)/c_T) + (D/D_k)]\} \quad (69)$$

The limiting cases are a function of the ratio of the molecular to Knudsen diffusion coefficients. The molecular regime is obtained when $D << D_k$ or $D/D_k \rightarrow 0$, and it may be seen by inspection that Eq. (40) is recovered from Eq. (69) when this substitution is made.

The other limiting case is most clear when the approximations $c_{ox}(0) \approx \chi c_T$ and $c_{ox}(\xi) \approx 0$ are made. With these, Eq. (68) may be rewritten as

$$k_p' = (4Dc_T/N) \ln\{[(1 + \chi)(D_k/D) + 1]/[(D_k/D) + 1]\} \quad (70)$$

In the Knudsen regime, D_k/D is small and k_p' may be validly approximated, using $\ln(1 + x) \approx x$, for small x, as

$$k_p' \approx (4Dc_T/N)\{(1 + \chi)(D_k/D) - (D_k/D)\} \approx (4D\chi c_T/N)(D_k/D) = 4\chi(D_k c_T/N) \quad (71)$$

Thus, the value of k_p' in the Knudsen limiting case is differentiated from that in the molecular case, Eq. (59), by both the magnitude of the diffusion coefficient and numerical factor. The differences are small. The value of the numerical coefficient in the Knudsen case is higher than the molecular case because of the absence of intermolecular collisions that preclude convection effects. In a pure oxygen atmosphere, i.e., $\chi = 1$, the numerical coefficient in the Knudsen case is a factor of 1.69 larger than that in the molecular case, which tends to moderate the effect of the difference between D and D_k. As χ is reduced, the values of the numerical coefficients converge.

Since D_k is dependent on the dimensions of the pore, k_p' may be a function of, for example, interface thickness. It is possible to estimate the value of k_p' as a function of the characteristic dimension of the pore using Eq. (70). For O_2, D_k (m^2/s) is obtained from Eq. (64).

$$D_k = 8.575T^{1/2}d \quad (72)$$

c_T, in mol/m^3, is calculated from the ideal gas law,

$$c_T = P/(RT) = 1.203 \times 10^{-1}(P/T) \quad (73)$$

N was calculated assuming the density of carbon, which varies depending on the degree of crystallinity, to be 1.8 g/cm^3, or

$$N = \rho/M = 1.5 \times 10^5 \text{ mol/m}^3 \quad (74)$$

D, in m^2/s, can be estimated from Chapman–Enskog theory. A binary mixture of CO–O_2 was assumed in the calculation. From Eqs. (9), (10), and (11), and the values in Table I,

$$D = 1.593 \times 10^{-4}(T^{3/2}/P) \quad (75)$$

Combining these expressions with Eq. (70) gives

$$k_p' = 6.263 \times 10^{-10}T^{1/2} \ln\{((1 + \chi)4.392 \times 10^4(Pd/T) + 1)/(4.392 \times 10^4(Pd/T) + 1)\} \quad (76)$$

A family of three curves generated using this function, with $\chi = 1$ (1 atm pure O_2), are shown in Fig. 3. Two variables are explored: temperature and pressure. It is evident that temperature only weakly affects the magnitude and shape of the curve. In the molecular (large d) regime, D is proportional to $T^{3/2}$ and c_T is inversely proportional to temperature, so k_p', is directly proportional to the square root of temperature. At 1 atm pressure, the limiting values in the molecular regime are calculated to be 1.42×10^{-8} and 1.55×10^{-8} m^2/s, for 800° and 1000°C, respectively; i.e., the difference is less than 10%. These values for k_p predict recession of 1 cm in roughly 2 h—7030 and 6460 s, respectively. The temperature effect in the Knudsen regime is also modest, but, interestingly, it is of opposite sign because D_k has a weaker temperature dependence, $T^{1/2}$, than D. In this regime, k_p is inversely proportional to the square root of temperature; at higher temperatures, k_p is smaller.

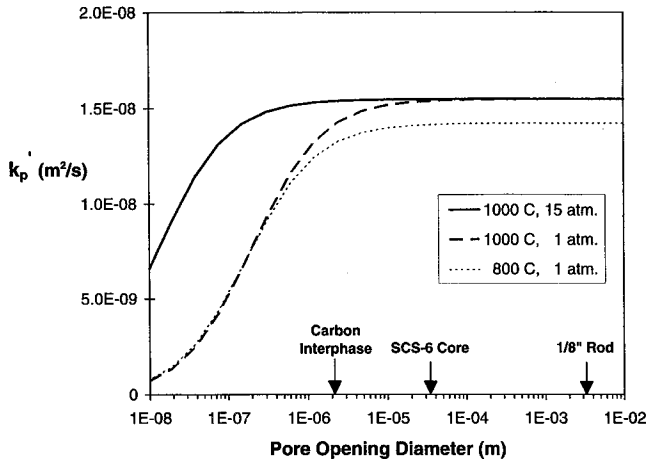

Fig. 3. Effect of variations in temperature and pressure on the parabolic rate constant, k_p (assuming $O_2 + 2C \rightarrow 2CO$).

Secondly, a reduction in the pore opening diameter, d, to 10 μm is predicted to produce almost no effect for any of the three cases considered. More importantly, the magnitude of Knudsen effects is always small; at 1000°C and 1 atm pure O_2, when "d" is 1 μm, k_p' is 80% $k_p'(\infty)$ and when "d" is 0.1 μm (which is the thickness often quoted as the minimum permissible for desirable mechanical properties in CFCCs[19]) $k_p'(0.1)/k_p'(\infty)$ is 1/3. Finally, increasing pressure does not change the value of k_p' in the molecular regime, because the direct proportionality of c_T is nullified by the inverse proportionality of D. However, at higher pressures the already modest Knudsen effects are further suppressed (at 15 atm and d = 0.1 μm, k_p' and $k_p'(\infty)$ differ by less than 2%).

III. Experimental Procedure

Oxidation experiments using two model composite systems were conducted. Each consists of a carbon cylinder in a nonreactive matrix. Schematic cross sections of each are shown in Fig. 4. The two are principally distinguished by the type of carbon and 2 orders of magnitude difference in diameter. These diameter values are indicated on the scale in Fig. 3. It can be seen that k_p for these two systems should be indistinguishably close. Further, either system gives a k_p that closely approximates the value expected for a 2 μm thick interphase. (i.e., <20% different), provided the ambient pressure is held constant at 1 atm. Thus, the analytical model allows results from model systems to be applied to carbon recession in composites, where carbon is used either as a fiber or interphase.

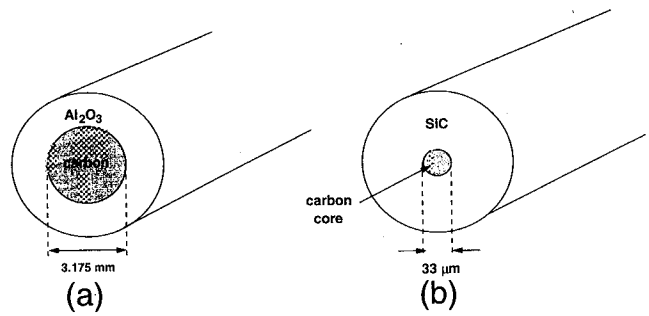

Fig. 4. Schematics of model microcomposites used in oxidation experiments: (a) carbon rod in Al_2O_3, (b) pitch-based carbon in silicon carbide sheath (SCS-6 fiber).

The first model system was constructed by inserting 3.175 mm (1/8 in.) diameter carbon rods into hollow alumina cylinders. The rods are commercially available (E. F. Fullum, Schenectady, NY) and commonly used as electrodes for preparing physically vapor deposited carbon films. Both the rods and the alumina had initial lengths of nominally 65 mm. Individual assemblies were exposed at temperatures in the range of 700° to 1200°C and for times to 24 h in a muffle furnace. Following exposure, the carbon rod was removed from the alumina sheath and the dimensions were measured. The recession distance was calculated by halving the difference between the length of the alumina tube and that of the carbon rod after exposure. In all cases, the diameter of the rod remained unchanged, within the resolution of a high-quality micrometer.

The second model system was an SCS-6 fiber (Textron Specialty Materials, Lowell, MA) which has a ~33 μm diameter pitch-based carbon core within a SiC sheath. Both the carbon core and the CVD SiC sheath have been well characterized using transmission electron microscopy.[20,21] The carbon core consists of a random mixture of small (1–50 nm) turbostatic carbon blocks. The SCS-6 fibers were exposed at two temperatures, 800° and 1000°C. At these temperatures, oxidation of the SiC sheath should be negligible.[22] Fiber lengths from 2.5 to 12 cm, depending on the anticipated recession distance, were used. The furnace was heated rapidly to temperature and the specimens were held at the desired temperature for times to 50 h. For the longest fibers, the equilibrium temperature was ~10°C lower at the ends than the center. The samples were removed after cooling the furnace to room temperature.

Following exposure, the recession lengths of the carbon cores were measured. The details of how this was accomplished are summarized elsewhere.[23] In short, the measurements were accomplished by mounting a section of the fiber on a plate with epoxy and grinding to approximately one-half of its original diameter. The recession length of the carbon core could then easily be measured using optical microscopy. Figure 5 shows typical optical micrographs of a ground fiber following 2 h of oxidation at 800°C. In both model systems, the receded carbon surface was planar following oxidation at high temperature or long times. However, at lower temperatures and shorter times, the carbon had a pointed morphology, as seen in the figure. In these cases, recession distances were recorded from the end of the sheath to the tip of the receded carbon.

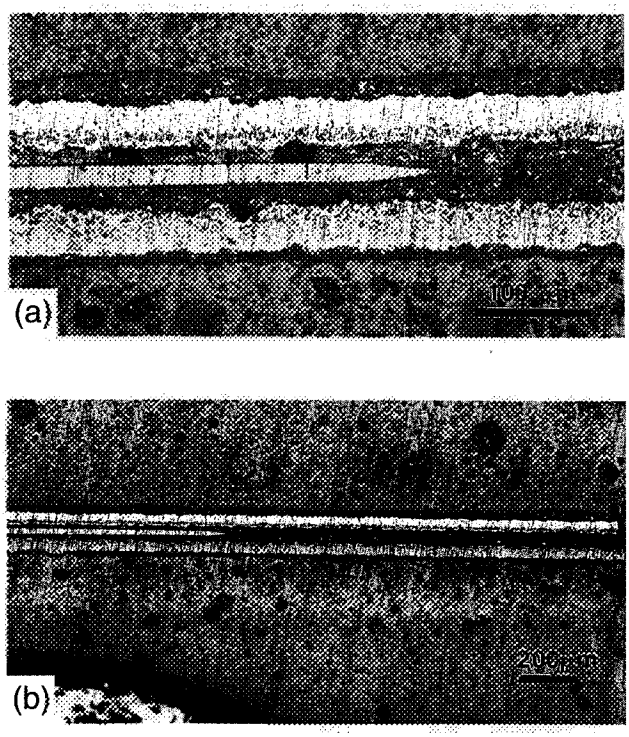

Fig. 5. Optical micrographs of sectioned and polished SCS-6 fiber oxidized for 2 h at 800°C.

Solely for experimental convenience, the two systems were oxidized under different atmospheric conditions, the carbon rods in nominally static air and the SCS-6 in flowing (~6 cm/s) oxygen. In both, the atmosphere external to the pore is well mixed. In the case of nominally static air, this is due to thermal convection. The ambient pressure was the same in all experiments (1 atm). Therefore, the only difference of significance is the value of χ, which is either 0.2 or 1.

Reproducibility of the data was checked in two ways. On the SCS-6 fibers, measurements from both ends of each oxidized fiber were taken and found to be consistent. In both model composite systems, selected experiments were repeated, and again a high degree of consistency was observed.

IV. Results

Predictions for recession distances in the two very different microcomposite systems were calculated using the linear-parabolic relationship of Eq. (1). It was assumed that the reaction was CO, and k_p was calculated using Eq. (76) with appropriate values for d, χ, T, and P. The linear rate constant is dependent on the physical and chemical characteristics of the carbon being oxidized; a different k_l is required for each system, and can be obtained only by fitting experimental data.

For the carbon rod, it was determined that k_l was so large that the recession behavior was accurately modeled as purely parabolic. Figure 6 presents both the experimental data and curves calculated for the corresponding temperatures using Eq. (76). It can be seen that the model, which has no adjustable parameters, gives very accurate predictions. For this system, recession rate depends very weakly on temperature, as expected, since it is controlled by gas phase diffusion.

As mentioned in Section III, the receding interface did not always remain planar, but developed a pointed morphology at lower temperatures. The presence or absence of the pointed tip does not appear to affect the agreement between the model and the experimental data. This is not surprising. The principal effect of such a tip shape is to expose additional surface area for reaction, effectively increasing k_l, which is already apparently so large that it can be neglected.

Very different behavior was observed with the SCS-6 cores. Figure 7 shows a comparison of the experimental and predicted recession distances for the SCS-6 fibers at 800° and 1000°C. Again, the predicted recessions were calculated using Eq. (1) and obtaining k_p from Eq. (76). In this case, however, assuming purely parabolic behavior resulted in a gross overestimation of recession distances. In other words, the oxidation rate was slower than would be expected based on diffusion control, and oxidation must be limited, over a significant amount of time, by

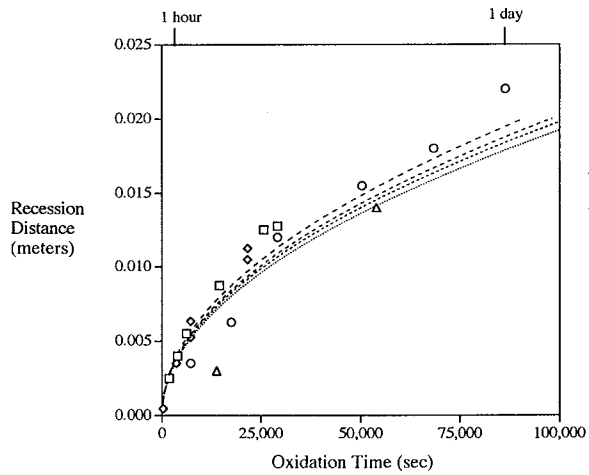

Fig. 6. Comparison of predicted recession distances to experimental observations for 3.175 mm diameter carbon rods in alumina sheaths (△ 775°C, ○ 900°C, □ 1000°C, ◇ 1200°C).

the chemical reaction at the receding carbon surface. The value of k_1 that gave the best fit to the 800°C data was 2.5×10^{-6} m/s.

V. Discussion

Carbon oxidation is, of course, generally recognized to be fast, but the general analytical model allows quantitative prediction of recession rates and important variables to be analyzed. It is perhaps most illuminating to initially consider the transition from linear to parabolic kinetics. Although it is recognized that the transition is broad (i.e., occurring over a wide range in time), it is possible to define the transition as the recession distance, or equivalently the oxidation time, at which the two terms on the left-hand side of Eq. (1) are equal. Equating these terms and substituting using Eqs. (6) and (59), i.e., assuming O_2 diffusion in and CO diffusion out, gives

$$\xi_{trans} = k_p/k_l = (4/\chi) \ln (1 + \chi)(D/K_r) \quad (77)$$

Thus, the transition occurs at a depth which depends on the type of carbon (through K_r), the partial pressure of oxygen, the total system pressure, and temperature. The transition depth for air ($\chi = 0.2$) is ~26% of the depth for pure O_2 ($\chi = 1$). The transition occurs earlier (smaller values of ξ_{trans}) at lower system pressure because k_l is proportional to pressure, but k_p (in the molecular regime) is independent of pressure. The temperature dependence is primarily through the exponential function, in K_r, and the transition is delayed (occurs at larger values of ξ_{trans}) at lower temperatures.

The fits to the experimental data allow transition distances to be estimated. For the case of the carbon rods, the transition distances are negligibly small at all temperatures investigated, on the order of 10 nm or less. During fitting it was observed that using k_l's small enough to correspond to larger transition distances caused poorer fits. In contrast, the SCS-6 cores were best fit using values of k_l that yield transition distances in excess of 5 cm at 800°C, and nearly 1 cm at 1000°C. Thus, it is entirely plausible for recession kinetics to fall into either of the two limiting cases of Eq. (1), for distances of engineering interest. It depends nearly entirely on the chemical and physical properties of the carbon.

The results of the analysis given in Section II can be summarized as follows. When the recession distance, ξ, is small, such that $\xi << \xi_{trans}$, the recession rate will be linear, inversely proportional to pressure, exponentially dependent on temperature, and the type of carbon will affect the oxidation rate. In the other limiting case, $\xi >> \xi_{trans}$, recession will be parabolic, independent of the type of carbon, and weakly dependent on temperature and the nature of the gas phase reaction sequence. Lastly, the parabolic recession rate will be independent of pressure in the molecular regime, but directly proportional to pressure in the Knudsen regime.

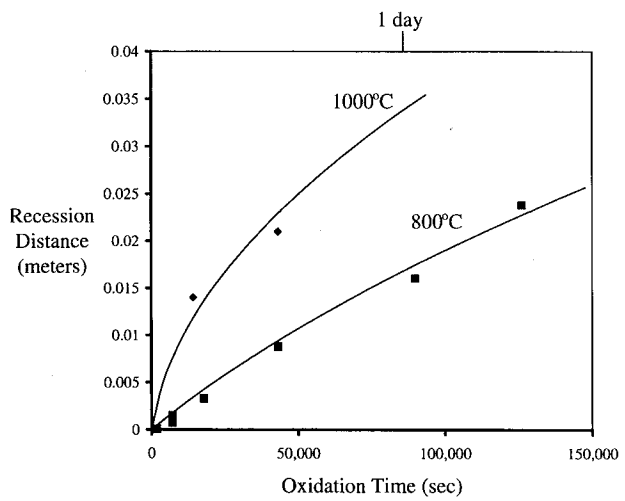

Fig. 7. Comparison of predicted recession distances to experimental observations for 33 μm carbon core in SCS-6 SiC sheath.

Knudsen effects are predicted to be very modest; i.e., carbon recession will be rapid even when the effective gas phase diffusion coefficient is D_k. Consider first the behavior anticipated for carbon coatings with thicknesses in the range of 0.1–1.0 μm. Referring to Fig. 3, it can be seen that though both oxidize more slowly than that predicted using the molecular approximation, the effect is small for both. The values of k_p at 1000°C and 1 atm for the 1.0 and 0.1 μm coatings are roughly 80% and 30%, respectively, of the molecular prediction. Although these values are lower, they do not qualitatively change the situation. Substitution of the reduced values for k_p into Eq. (77) still yields ξ_{trans} on the order of centimeters. Furthermore, if the ambient pressure is raised to 15 atm, the 1.0 μm coating falls completely into the molecular regime and the 0.1 μm coating is predicted to have a k_p suppressed by less than 15%, relative to the molecular case. Thus, in heat engine applications of composites, Knudsen effects are essentially of no consequence.

The fact that Knudsen diffusion is not slow has other important implications for composites. One class of alternate interface coatings is a multilayer approach in which concentric cylinders of carbon and silicon carbide are deposited. In such systems, the thickness of the carbon coatings is perhaps an order of magnitude thinner than simple coatings, on the order of tenths of micrometers rather than a few micrometers. One purported advantage of this approach is that the oxidation kinetics will be retarded. The above discussion makes it clear that reducing the thickness of the carbon to this range will not be sufficient to suppress oxidation to an acceptable rate.

Also, it is generally recognized that oxidation under stress of CFCCs is much more rapid than static oxidation. There are two possible contributors to an acceleration of oxidation: increasing the matrix-crack opening displacement and oxidant ingress into the debond region at the fiber interface.

Increasing the crack opening displacement is unlikely to be of much consequence for two independent reasons. First, the rate of recession will usually be controlled by the reaction at the receding carbon interface; thus, facilitating gas phase diffusion by opening the crack will not affect the rate. Second, even when recession is controlled by gas phase diffusion, the crack opening need only be modest, fractions of a micrometer, before the diffusion coefficient reaches the limiting value of the molecular regime.

Oxygen ingress into the debond region represents an interesting situation. When a matrix crack passes through a composite, the interface between the intact fibers which span the crack and the matrix is debonded over a finite distance. If the debonded region has a finite opening, gas phase diffusion will rapidly lead to oxidation along the length of the debond (even if the opening leads to diffusion in the Knudsen regime). This leads to an instability, because oxidation will decouple the matrix from the fiber, preventing stress transfer, which indirectly results in a further length of interface being debonded. The newly debonded region is then subject to oxidation and this repeats in a continuous cycle. It is plausible that this mechanism causes the generally observed strong coupling between stress and oxidation.

VI. Summary and Conclusions

Oxidation of carbon in model composites is well described by a linear-parabolic law. The parabolic constant, k_p, can be predicted using the kinetic theory of gases, whereas k_l must be determined by fitting experimental data. The consequences of

this work for conditions of engineering interest (800°C < T < 1200°C and recession distances ≤1 mm) and experimental studies are many. Whether CO or CO_2 is formed directly, or whether CO_2 is the reaction product of sequential oxidation reactions, is an unimportant consideration for most applications. For the case of a fiber-reinforced composite, it is unlikely that a carbon interphase can be fabricated thin enough to slow oxidation to a technologically acceptable rate. Once carbon is exposed to oxygen, via pores or matrix cracks, oxidation will proceed at a rapid rate, nearly independent of the magnitude of the pore/crack opening, the partial pressure of oxygen, or the total system pressure. The single, overriding, variable of consequence in moderating the kinetics is controlling the rate of chemical reaction at the receding carbon interface.

APPENDIX
List of Parameters Used in Model

Symbol	Definition	Units
c_T	Total concentration of gases	mol/m^3
c_i	Concentration of specie i at distance x	mol/m^3
$c_{ox}(0)$	Concentration of oxygen in the environment	mol/m^3
$c_{ox}(\xi)$	Concentration of oxygen at carbon/gas interface	mol/m^3
d	Pore opening diameter	m
d'	Annular pore opening thickness	m
D_i	Molecular diffusivity of specie i	m^2/s
D_k	Knudsen diffusivity for oxygen	m^2/s
j_i	Flux of specie i	mol/m^2·s
K_r	Reaction rate constant	m/s
k_l	Linear recession rate constant	m/s
k_o	Preexponent in Arrhenius form of k_l	m/s
k_p	Parabolic rate constant for recession	m^2/s
M_i	Molecular weight of specie i	N/mol
N	Molar density of carbon	mol/m^3
P	Pressure of the environment	MPa
Q	Activation energy for carbon oxidation reaction	J/mol
r	Rate of reaction	mol/m^2·s
R	Gas constant	J/mol·K
t	Time	s
T	Absolute temperature	K
v_i	Velocity of the specie i	m/s
ε/k	Energy of molecular interaction normalized by Boltzmann's constant	K
σ_{ij}	Collision diameter for species i,j	m
Ω_{ij}	Collision integral (tabulated) for i,j	
j_i	flux of specie i	mol/m^2·s
x	Distance from the surface into the pore (Fig. 1)	m
ξ	Recession distance	m
χ	Fraction defining partial pressure of oxidant	

Acknowledgments: The development of metallographic techniques to measure recession distances in SCS-6 fibers is attributed to O. Unal. The authors also gratefully acknowledge the thoughtful comments of Nate Jacobson.

References

[1]T. Mah, T. A. Parthasarathy, K. Keller, and J. Guth, "Fugitive Interface Coating in Oxide–Oxide Composites: A Viability Study," *Ceram. Eng. Sci. Proc.*, **12** [9–10] 1802–18 (1991).

[2]J. M. Thomas, *Chemistry and Physics of Carbon*, Vol. 1, p. 135–68. Edited by P. L. Walker Jr. Marcel Dekker, New York, 1965.

[3]V. Z. Shemet, A. P. Pomytkin, and V. S. Neshpor, "High Temperature Oxidation Behavior of Carbon Materials in Air," *Carbon*, **31** [81] 1–6 (1993).

[4]D. W. McKee, "Borate Treatment of Carbon Fibers and Carbon/Carbon Composites for Improved Oxidation Resistance," *Carbon*, **24** [6] 737–41 (1986).

[5]K. L. Luthra, "Oxidation of Carbon/Carbon Composites—A Theoretical Analysis," *Carbon*, **26** [2] 217–24 (1988).

[6]S. Drawin, M. P. Bacos, J. M. Dorvaux, and O. Lavigne, "Oxidation Model for Carbon–Carbon Composites"; pp. 1112–22 in proceedings of the Fourth International Aerospace Planes Conference (Orlando, FL, 1992), Vol. 7, Paper No. 92-5016. American Institute for Aeronautics and Astronautics, Washington, DC, 1992.

[7]F. Lamouroux, G. Camus, and J. Thebault, "Kinetics and Mechanisms of Oxidation of 2D Woven C/SiC Composites: I, Experimental Approach," *J. Am. Ceram. Soc.*, **77** [8] 2049–57 (1994).

[8]F. Lamouroux, R. Naslain, and J.-M. Jouin, "Kinetics and Mechanisms of Oxidation of 2D Woven C/SiC Composites: II, Theoretical Approach," *J. Am. Ceram. Soc.*, **77** [8] 2058–68 (1994).

[9]L. Filipuzzi, G. Camus, R. Naslain, and J. Thebault, "Oxidation Mechanisms and Kinetics of 1D-SiC/C/SiC Composite Materials: I, An Experimental Approach," *J. Am. Ceram. Soc.*, **77** [2] 459–66 (1994).

[10]L. Filipuzzi and R. Naslain, "Oxidation Mechanisms and Kinetics of 1D-SiC/C/SiC Composite Materials: II, Modeling," *J. Am. Ceram. Soc.*, **77** [2] 467–80 (1994).

[11]K. L. Luthra, "Theoretical Aspects of the Oxidation of Silica-Forming Ceramics"; to be published in Proceedings of NATO Advanced Research Workshop (Tubingen, Germany, Aug. 30–Sept. 3, 1993).

[12]J. Bernstein and T. B. Koger, "Carbon Film Oxidation-Undercut Kinetics," *J. Electrochem. Soc.*, **135** [8] 2086–90 (1988).

[13]J. A. DiCarlo; private communication. NASA Lewis Research Center, Cleveland, OH, 1993.

[14]R. T. Bhatt, "Oxidation Effects on the Mechanical Properties of a SiC-Fiber-Reinforced Reaction-Bonded Si_3N_4 Matrix Composite," *J. Am. Ceram. Soc.*, **75** [2] 406–12 (1992).

[15]S. I. Rokhlin, Y. C. Chu, A. I. Laventyev, G. Y. Baaklini, and R. T. Bhatt, "Ultrasonic Assessment of Oxidation Damage in SiC/RBSN Composites," *Ceram. Eng. Sci. Proc.*, **15** [5] 1164–73 (1994).

[16]B. E. Deal and A. S. Grove, "General Relationship for the Thermal Oxidation of Silicon," *J. Appl. Phys.*, **36** [12] 3370–78 (1965).

[17]W. Geankoplis, *Mass Transport Phenomena*; pp. 27–28, 151–53. Ohio State University Bookstores, Columbus, OH, 1978.

[18]R. B. Bird, W. E. Stewart, and E. N. Lightfoot, *Transport Phenomena*; pp. 496–501. Wiley, New York, 1960.

[19]P. F. Tortorelli, S. Nijhawan, L. Riester, and R. A. Lowden, "Influence of Fiber Coatings on the Oxidation of Fiber-Reinforced SiC Composites," *Ceram. Eng. Sci. Proc.*, **14** [7–8] 358–66 (1993).

[20]X. J. Ning and P. Pirouz, "The Microstructure of SCS-6 Fiber," *J. Mater. Res.*, **6** [10] 2234–48 (1991).

[21]X. J. Ning, P. Pirouz, K. P. D. Lagerlof, and J. DiCarlo, "Structure of Carbon in Chemically Vapor Deposited SiC Monofilaments," *J. Mater. Res.*, **5** [10] 2865–76 (1990).

[22]J. A. Costello and R. E. Tressler, "Oxidation Kinetics of Silicon Carbide Crystals and Ceramics: I, In Dry Oxygen," *J. Am. Ceram. Soc.*, **69** [9] 674–81 (1986).

[23]J. D. Cawley, O. Unal, and A. J. Eckel, "Oxidation of Carbon in Continuous Fiber Reinforced Ceramic Matrix Composites"; pp. 541–52 in Ceramic Transactions, Vol. 38, *Advances in Ceramic Matrix Composites*. Edited by N. P. Bansal. American Ceramic Society, Westerville, OH, 1993. □